CORE
Metadata, citation and similar papers at core.ac.uk
Provided by Kanazawa University Repository for Academic Resources

Bend formability and strength of Cu-Be-Co alloys

著者	Monzen Ryoichi, Hosoda Takasumi, Takagawa Yusaku, Watanabe Chihiro
journal or publication title	Journal of Materials Science
volume	46
number	12
page range	4284-4289
year	2011-06-01
URL	http://hdl.handle.net/2297/26234

doi: 10.1007/s10853-010-5232-7

Bend Formability and Strength of Cu-Be-Co Alloys

Ryoichi Monzen · Takasumi Hosoda · Yusaku Takagawa · Chihiro Watanabe

R. Monzen · C. Watanabe

Division of Innovative Technology and Science, Kanazawa University, Kakuma-machi, Kanazawa 920-1192, Ishikawa, Japan

T. Hosoda · Y. Takagawa

Division of Mechanical Systems Engineering, Kanazawa University, Kakuma-machi, Kanazawa 920-1192, Ishikawa, Japan

Abstract The effects of addition of 0.01 and 0.03wt.%Mg on the bend formability and strength of a Cu-1.8wt.%Be-0.21wt.%Co alloy aged at 320°C for 30 min have been investigated metallographically. The addition of Mg to the Cu-Be-Co alloy enhances the bend formability and strength of the alloy. The enhancement of strength is caused by the increase in volume fraction of γ'_I precipitates in the Cu matrix. In bending of the alloys with and without 0.01 and 0.03wt.%Mg, a number of micro necks first arise along grain boundaries, and part of them grows, resulting in surface wrinkles, which finally lead to surface cracking. The cracking is initiated from voids formed by destruction of bar-like γ precipitates in discontinuous precipitation (DP) cells and propagates along grain boundaries. The addition of Mg decreases the width of DP cells, resulting in better bend formability. This arises because smaller stress concentration due to less inhomogeneous deformation develops in cells and, as a result, destruction of the γ precipitates in cells occurs less easily as the cell width decreases.

Keywords: copper-beryllium alloy, bend formability, strength, discontinuous precipitation, magnesium addition

Introduction

Age-hardened Cu-Be-Co system alloys have the highest hardness and tensile strength among Cu-base alloys, and high electrical conductivity. The alloys, therefore, are widely used in such applications as electrical connectors and small springs. These applications require not only high strength and conductivity but also good bend formability. However, there have been few studies on bend formability of the Cu-Be-Co alloys. The addition of a slight amount of Co to a Cu-Be alloy aims to suppress discontinuous precipitation (DP) reactions [1]. Chiba et al. [2] have examined the relationship between the bend formability and aging condition of an under-aged Cu-1.91wt.%Be-0.21wt.%Co alloy, and shown that the presence of DP cells may have a bad influence on the bend formability. On the other hand, it has been reported that the addition of a slight amount of Mg to a Cu-Be alloy suppresses formation of DP cells and also improves strength of the alloy [3, 4]. It may thus be expected that the addition of Mg to a Cu-Be-Co alloy enhances not only the strength but also the bend formability of the alloy.

We have found that adding 0.01 and 0.03wt.%Mg to a Cu-1.8wt.%Be-0.21wt.%Co alloy aged at 320°C for 30 min improves the strength of the alloy, and reduces the width of DP cells, resulting in better bend formability. In this study, the causes for these improvements will be examined metallographically.

Experimental procedure

Cu-1.8wt.%Be-0.21wt.%Co, Cu-1.8wt.%Be-0.21wt.%Co-0.01wt.%Mg and Cu-1.8wt.%Be-0.21wt.%Co-0.03wt.%Mg alloys were prepared by melting in an Argon atmosphere. The cast alloys were homogenized at 860°C for 24h in a vacuum and then cold-rolled to a 50% reduction in thickness. The rolled strips were solutionized at 800°C for 20min in an Argon atmosphere and then water quenched. The solutionized alloys were cold-rolled to 10% reduction in thickness and then aged at 320°C for 30min in the Argon atmosphere. This aging condition was selected since Cu-base alloys containing about 2.0%Be and 0.2%Co are industrially aged at 320°C for a time between 15 and 30min.

Microhardness tests were carried out using the Vickers method. The indentation was

made on the well-polished surface of the specimen pieces with a diamond square-based pyramid under a load of 0.3kg for a period of 20s. Tensile tests were performed using a static Instron type testing machine with a constant strain rate of $10^{-3}s^{-1}$ at room temperature. Electrical resistivity measurements were made by a Hocking AutoSigma 3000 electrical conductivity tester at 20ºC. Transmission electron microscopy (TEM) was performed using a JEOL 2010FEF and a Hitachi H-9000NAR microscope at operating voltages of 200kV and 300kV, respectively. Thin foils for TEM observations were prepared using a twin-jet polishing method with a solution of 67% methanol and 33% nitric acid at -20ºC and 5V.

The 90º W-bend tests were carried out according to the literature [5]. 20, 40 and 60º bend tests were also performed. The aged specimens for the bend tests had a dimension of $30^{l} \times 10^{w} \times 0.25^{t}$ mm^3 and the bend axis was perpendicular to the direction of rolling. After the bend tests, the outer surface of the specimen pieces was observed using an optical microscope and a scanning electron microscope, and bend formability of the specimens was judged from the literature [5].

Results and discussion

Effect of Mg on strength

The hardness changes of Cu-1.8%Be-0.21%Co and 0.01 and 0.03%Mg-added Cu-1.8%Be-0.21%Co alloys were examined during aging at 320ºC. The addition of 0.01 and 0.03%Mg did not significantly change the microhardness after the solution treatment at 800ºC for 20min and subsequent 10% cold-rolling. For each alloy, the peak hardness effect occurs on aging for about 3h, and the hardness continues to decrease with further aging. The addition of 0.01 and 0.03%Mg slightly increased the hardness throughout the aging process.

Aging the present alloys at 320ºC for 30 min produced disk-shaped precipitates parallel to $\{100\}_\alpha$ of the Cu matrix. Figure 1 depicts a high-resolution (HR) TEM image of the precipitates, taken using the electron beam parallel to the $[110]_\alpha$ direction. The precipitates have a structure of alternate Be and Cu matrix layers parallel to $(001)_\alpha$. The precipitates labeled A and B are composed of four Be-layers. Lattice fringes nearly parallel to $(1\bar{1}0)_\alpha$ also

are visible. The average spacings of the lattice fringes, corresponding to the $(001)_p$ ($//(001)_\alpha$) and $(010)_p$ ($\cdot//\cdot(1\bar{1}0)_\alpha$) planes of the precipitates, were measured as c=0.32 nm and b=0.25nm. About thirty precipitates, consisting of four Be-layers, viewed along the $[110]_\alpha$ zone axis were examined. The angle α between $[010]_p$ and $[001]_p$ was 87º on average. These values are in good agreement with the values of b=0.254, c=0.324 nm and α=87º for the γ'_I phase, previously reported [6]. In the present alloys, there primarily existed γ'_I precipitates, consisting of four Be-layers. DP cells were also observed at grain boundaries, as exemplified in Fig. 2. The DP cell is composed of lamellae of the equilibrium γ phase (CuBe intermetallic) and solute-depleted α phase (Cu-rich solid solution).

Table 1 lists the tensile properties and electrical conductivity of the Cu-Be-Co and the Mg-added alloys aged at 320 ºC for 30 min. The 0.2% proof stress and tensile strength increase with increasing the amount of Mg. On the other hand, the addition of Mg does not essentially affect the elongation and electrical conductivity.

Since the γ'_I precipitates have the structure of alternate Be and Cu layers parallel to $\{100\}_\alpha$, glide dislocations can cut through them. It is well known that the yield stress of a precipitation-strengthened alloy containing precipitates which can be cut through by glide dislocations at room temperature is controlled by the dislocation shearing mechanism at an under-aging condition and by the Orowan dislocation looping mechanism at an over-aging condition [7, 8]. It will be examined whether the yield stress of the present alloys under-aged at 320ºC for 30 min is governed by the shearing mechanism or Orowan mechanism. For comparison, the alloys peak-aged at 320ºC for 3h will also be investigated. In the peak-aged alloys, γ' precipitates, much larger than γ'_I precipitates, were observed within the grain interiors. The γ' phase heterogeneously precipitates on the γ_I phase, which has the structure of alternate Be and Cu layers parallel to $\{100\}_\alpha$, and appears following the γ'_I phase [6]. The present alloy specimens under-aged (UA) and peak-aged (PA) were elongated by about 2% strain, then annealed at 200 ºC for 3 h and again elongated. The result for the UA and PA Cu-Be-Co specimens is presented in Fig. 3. The PA specimen shows larger work-hardening and larger softening on annealing after work hardening than the UA specimen. The same tendency held for the Mg-added alloys. Large work-hardening in an initial stage of deformation and softening on annealing at a relatively low temperature after work hardening

are characteristic of a dispersion-strengthened alloy. The large work hardening is caused by the back stress in the matrix produced by Orowan loops around particles, and the softening on low-temperature annealing is attributed to climbing and disappearance of the Orowan loops, responsible for the back stress, by pipe diffusion [9, 10]. Thus it can be concluded that the yield stress of the present UA alloys is governed by the shearing mechanism.

When the yielding occurs by the shearing mechanism, the increase in yield stress is written as [7]

$$\Delta\sigma \propto (f \cdot r)^{1/2}, \quad (1)$$

where f and r are the volume fraction and radius of spherical precipitates. Table 2 lists the radius and volume fraction of disk-shaped γ'_I precipitates in each alloy. The volume fractions were determined by applying the electrical resistivities of the UA alloys to the experimental data on the dependence of the electrical resistivity on the Be concentration in the literature [11]. As the amount of Mg increases, the radius does not significantly change but the volume fraction increases. Therefore, the increase in strength by the Mg addition can be ascribed to the increase in volume fraction of γ'_I precipitates.

Effect of Mg on bend formability

Table 3 summarizes the 0.2% proof stress, bend formability after the 90^o W-bend tests and width of DP cells for the Cu-Be-Co and 0.01 and 0.03% Mg-added alloys aged at 320°C for 30 min. The bend formability for the Mg-free, 0.01%Mg-added or 0.03%Mg-added alloy was judged as D, C or C, according to the literature [5]. It is evaluated by A, B, C, D and E, and is lowered in order of A, B, C, D and E [5]. When cracks are observed in the outer surface of a specimen, the bend formability is judged as D or E. (For example, in Fig. 4(c) it is evaluated as D.) There are grooves in the specimen surface for B or C (see Fig. 4(b)), and no grooves are formed for A. In Table 3, the addition of Mg decreases the width of DP cells and improves the bend formability. It is known that, in general, the higher the strength is, the further the bend formability is lowered. In the present study, however, in spite of the addition of 0.01 and 0.03%Mg enhances the strength, the bend formability is improved.

The first critical step of the DP reaction in Cu–Be alloys is heterogeneous grain

boundary nucleation [12, 13]. About 50 grain boundaries in each of the Cu-Be-Co and 0.01 and 0.03%Mg-added alloys aged at 320°C for 30 min were observed using TEM. Similar to our previous observation [13], precipitation of the γ phase took place first at grain boundaries and then the boundaries migrated. DP cells were formed for about 100, 80 and 50% of the boundaries examined in the Cu-Be-Co and 0.01 and 0.03wt.%Mg-added alloys, indicating that the addition of Mg suppresses the formation of cells. This qualitatively explains the decrease in cell width by the Mg addition in Table 3.

During bending deformation, a number of micro necks were first observed in the outer surface of specimens. Then, part of them grew, resulting in surface grooves, which finally led to surface cracking. This can be seen in Fig. 4, which shows the outer surface appearances of the same area after (a) 20°, (b) 40° and (c) 60° W-shape bend tests of an aged Cu-Be-Co specimen. The Mg-added alloys also exhibited similar surface appearances during bending deformation up to 90° W-shape bending: i.e., a lot of micro necks first arise and part of them grows, resulting in wrinkle grooves. However, the surface cracking was not formed after the 90° W-shape bending. The process until the formation of surface cracking is similar to that reported by Nagayoshi et al. [14] during bending deformation of a Cu-4wt.%Ni-1wt.%Si-0.02wt.%P alloy.

Figure 5 depicts a scanning electron microscopy (SEM) image after a 40° W-shape bend test of an aged Cu-Be-Co specimen. One can see cracks along grain boundaries, which were observed as the grooves by optical microscopy (Fig. 4(b)). In order to examine the cause for the crack formation, the Cu-Be-Co and the Mg-added alloys were observed by SEM after 20° and 40° W-shape bend tests, respectively and subsequent etching using a solution of water : ammonia water : hydrogen peroxide = 14 : 5 : 1 in volume ratio. The SEM observations revealed that voids were produced by destruction of bar-like γ precipitates in DP cells, as exemplified in Fig. 6. Therefore, it is said that the cracking starts from the formation of voids by the destruction of γ precipitates and progresses along grain boundaries.

Since the γ precipitates in cells are much coarser than the γ'_I precipitates in grains, as seen in Figs. 1 and 2, the strength of cells is lower than that of in-grains. It may hence be predicted that plastic deformation preferentially occurs in the α phase of cells during bending deformation, and thus stress concentration develops in the cells. Since thin foils for TEM

observation could not be prepared after bend tests, TEM foils were prepared from the three alloy specimens, aged at 320°C for 30 min and then cold-rolled to 10% reduction in thickness. Figure 7 depicts a TEM image of a cell in the cold-rolled Cu-Be-Co specimen. The density of dislocations in the cell is higher than that in the immediate vicinity of the cell. Analyses of selected-area electron diffraction patterns and Kikuchi lines for the Cu-Be-Co specimen revealed that there was a misorientation of about 3° on average between the in-cell and its vicinity. For the 0.01 and 0.03%Mg-added alloys, the respective misorientations of about 1 and 0° were found using the same method. That is, less inhomogeneous deformation develops in cells as the cell width decreases. This is also supported by the fact that, after the 20° W-shape bend tests, the destruction of the γ precipitates in cells was observed for the Cu-Be-Co alloy, whereas no destructed γ precipitates were noticed for the Mg-added alloys. Therefore, the improvement of bend formability due to the decrease in cell width can be attributed to the development of smaller stress concentration due to less inhomogeneous deformation in smaller cells and, as a result, the less easy formation of voids by the destruction of bar-like γ precipitates in the cells.

Conclusions

A metallographical investigation of the bend formability and strength of Cu-1.8wt.%Be-0.21wt.%Co alloys with and without 0.01 and 0.03wt.%Mg under-aged at 320°C for 30 min has yielded the following conclusions:

(1) The strength of the Cu-Be-Co alloy increases with increasing the amount of Mg addition. The Mg addition increases the volume fraction of γ'_I precipitates in the Cu matrix, resulting in the increase in strength.

(2) During bending deformation of the three alloys, a number of micro necks first arise in the vicinity of grain boundaries, and part of them develops into the grooves of wrinkles, which finally lead to surface cracking. The cracking begins at voids formed by destruction of bar-like γ precipitates in discontinuous precipitation (DP) cells and progresses along grain boundaries.

(3) The width of DP cells decreases as the amount of Mg addition increases. The decrease in

cell width brings about better bend formability. This can be ascribed to less easy formation of the voids by destruction of the γ precipitates, caused by the development of smaller stress concentration due to less inhomogeneous deformation in cells.

Acknowledgement A part of this work was conducted in the Kyoto-Advanced Nanotechnology Network, supported by the “Nanotechnology Network” of the Ministry of Education, Culture, Sports, Science and Technology (MEXT), Japan.

References

1. Williams DB, Butler EP (1981) Int. Met. Rev. 26:153.

2. Chiba H, Muramatsu N, Takeda M (2006) J Japan Res Inst Cu 45:76

3. Sugiyama M, Furukawa T (1964) J Japan Inst Metals 28:530

4. Murakami Y, Yoshida H, Kawashima T, Yamamoto S (1966) J Japan Inst Metals 30:508

5. Standard test method of bend formability for sheets and strips of copper and copper alloys in "JCBA (Japan Copper and Brass Association) technology standards" (JCBA, Tokyo, 2007)

6. Monzen R, Seo T, Sakai T, Watanabe C (2006) Mater Trans 47:2925

7. Gerold V, Haberkorn H (1966) Phys Status Solidi 16:675

8. Nagamura M, Ochiai S, Uehara T (1984) J Japan Inst Light Metals 34:517

9. Mori T, Osawa T (1979) Philos Mag 40:445

10. Monzen R, Kawaguchi Y, Mori T (1982) Acta Metall 30:965

11. Pawlek F, Reichel K (1956) Z Metallkde 47:347

12. Baumann SF, Michael J, Williams DB (1981) Acta Metall 29:1343

13. Monzen R, Watanabe C, Mino D, Saida S (2005) Acta Mater 53:1253

14. Nagayoshi H, Nishijima F, Watanabe C, Monzen R, Hara T (2006) J Japan Inst Metals 70:750

Figure and Table Captions

Fig. 1 HRTEM image of γ'_I precipitates in a Cu-1.8wt.%Be-0.21wt.%Co alloy aged at 320 °C for 30 min. The zone axis is parallel to $[110]_\alpha$.

Fig. 2 TEM image of a DP cell in a Cu-1.8%Be-0.21%Co alloy aged at 320 °C for 30 min.

Fig. 3 Stress-strain curves before and after annealing at 200 °C for 3 h for Cu-1.8%Be-0.21%Co specimens aged at 320 °C for 30 min (UA) and for 3 h (PA).

Fig. 4 Optical microscopy images showing the surface appearances of the same area after (a) 20°, (b) 40° and (c) 60° W-shape bending tests of a Cu-1.8%Be-0.21%Co alloy aged at 320°C for 30 min.

Fig. 5 SEM image showing the surface appearance after a 40° W-shape bending test of a Cu-1.8%Be-0.21%Co alloy aged at 320°C for 30min.

Fig. 6 SEM image of a void formed by destruction of a γ precipitate in a DP cell after a 20° W-shape bending test and subsequent etching of a Cu-1.8%Be-0.21%Co alloy aged at 320 °C for 30min.

Fig. 7 TEM image of a DP cell in a Cu-1.8%Be-0.21%Co alloy rolled to 10% reduction after aging at 320 °C for 30min.

Table 1 Mechanical properties and electrical conductivity of a Cu-1.8wt.%Be-0.21wt.%Co alloy and 0.01 and 0.03wt.%Mg-added alloys aged at 320°C for 30min.

Table 2 0.2% proof stress, and radius and volume fraction of disk-shaped γ'_I precipitates in a Cu-1.8%Be-0.21%Co alloy and 0.01 and 0.03%Mg-added alloys aged at 320°C for 30min.

Table 3 0.2% proof stress, bend formability and DP cell width for a Cu-1.8%Be-0.21%Co alloy and 0.01 and 0.03%Mg-added alloys aged at 320°C for 30min.

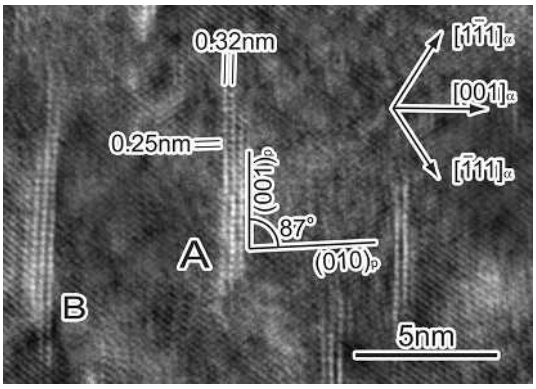

Fig. 1

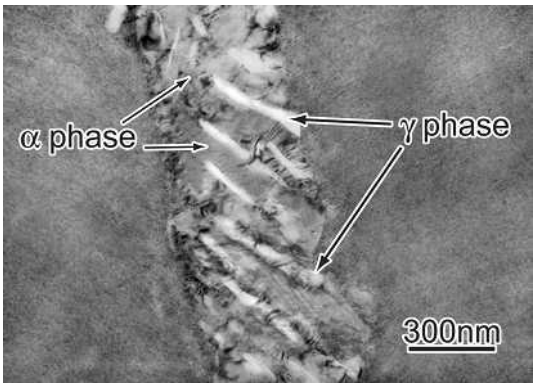

Fig. 2

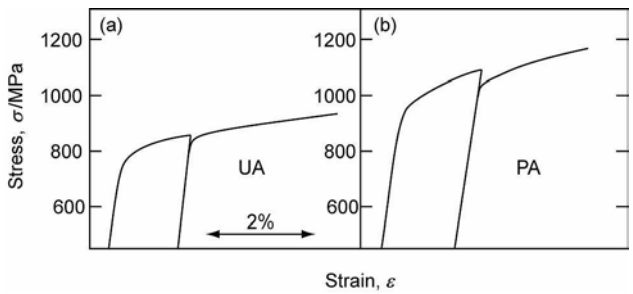

Fig. 3

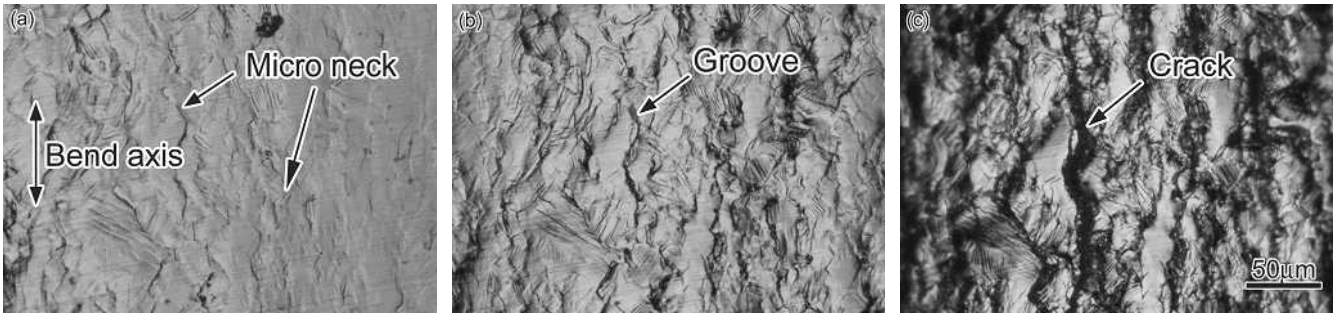

Fig. 4

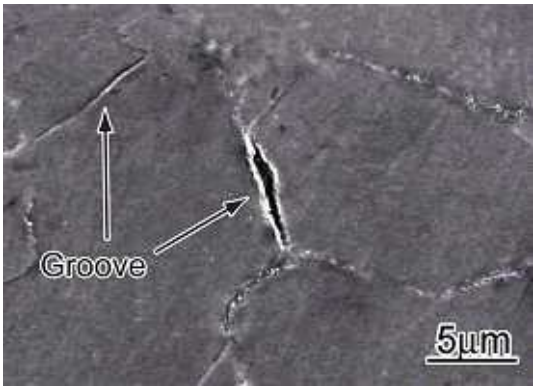

Fig. 5

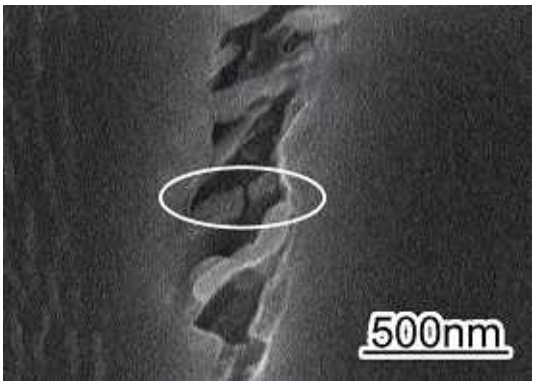

Fig. 6

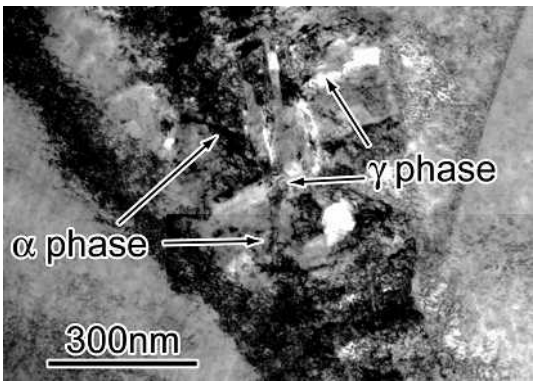

Fig. 7

Table 1

Alloy(wt%)	0.2% proof stress (MPa)	Tensile strength (MPa)	Elongation (%)	Electrical conductivity (%IACS)
Cu-Be-Co	770	960	11	20
Cu-Be-Co-0.01Mg	790	990	11	20
Cu-Be-Co-0.03Mg	840	1030	11	21

Table 2

Alloy	0.2% proof stress (MPa)	Radius (nm)	Volume fraction (%)
Cu-Be-Co	770	5.5	1.3
Cu-Be-Co-0.01Mg	790	5.5	1.4
Cu-Be-Co-0.03Mg	840	5.6	1.6

Table 3

Alloy	0.2% proof stress (MPa)	Bend formability	DP cell width (nm)
Cu-Be-Co	770	D	470
Cu-Be-Co-0.01Mg	790	C	240
Cu-Be-Co-0.03Mg	840	C	140